INSTITUTE OF PHYSICS PUBLISHING JOURNAL OF MICROMECHANICS AND MICROENGINEERING

J. Micromech. Microeng. **16** (2006) 1181–1188 doi:10.1088/0960-1317/16/7/010

Investigation of sidewall cracking in PMMA LIGA structures

L L Hunter[1], D M Skala[1] and B S Levey[2]

[1] Sandia National Laboratories, PO Box 969, Livermore, CA 94551-0969, USA
[2] University of Michigan, Ann Arbor, MI 48109, USA

E-mail: llhunte@sandia.gov

Received 2 March 2006, in final form 5 April 2006
Published 3 May 2006
Online at stacks.iop.org/JMM/16/1181

Abstract

During x-ray exposure in the LIGA process, the polymethylmethacrylate (PMMA) photoresist undergoes chain scission, which reduces the molecular weight of the exposed materials. Under some exposure and development conditions, sidewall cracking is observed on the PMMA sidewall, creating surface texture that is undesirable. In this research, exposed and developed PMMA sidewalls were examined for evidence of crack formation using optical profilometry. PMMA thickness, exposure dose and delay time between the end of exposure and beginning of development were varied. Our analysis of samples, with three different radiation doses and four different delay times from the end of exposure to the beginning of development, indicate that the first occurrence of cracking and the extent of cracking are affected by both the dose and the development delay time. This work includes the examination of the depth of cracks into the PMMA, distance between cracks, the width of cracks and the relationship between crack occurrence and dose profile. An empirical predictive model to correlate the delay time to the observance of sidewall cracking based on the deposited dose is presented. This information has direct implication for predicting processing conditions and logistics for LIGA fabricated parts.

1. Introduction

LIGA is a German acronym for lithography, electroplating and molding and describes a process used for creating parts with features sizes between 0.5 μm and 20 mm, typical [1]. With this process, high aspect ratio features with very straight sidewalls can be fabricated, making it ideal for a variety of parts that cannot be made using any other processes. The LIGA process consists of multiple steps including x-ray mask fabrication, substrate preparation, x-ray exposure, development of the exposed photoresist, electroplating into the photoresist mold and polishing of final parts. The resultant metal parts remain on the base substrate for use as a functioning device or are released for use as discrete parts. For mold inserts, the parts may remain on the base substrate or the mold may be overplated and machined to form a monolithic mold insert [2]. The quality of the metal sidewalls can have a large effect on performance, especially in optical and molding applications.

Ideally, the metal sidewalls have minimal average roughness over the entire feature, i.e. no sidewall defects, since any defect in the PMMA sidewall is replicated in the metal part or mold. Roughness that is present in PMMA sidewalls can be attributed to two primary causes: the quality of the mask and the exposure/development conditions [3]. Mask imperfections result in vertical striations that are parallel to the incident x-rays; these may have peak to valley variations up to several micrometers depending on fabrication techniques and resist quality. For example, there can be design and stitching errors in e-beam written patterns on the order of tens to hundreds of nanometers while particulate contamination on UV masks may cause micrometer-scale roughness on line edges [4–6]. Exposure and development conditions may also result in cracking throughout sidewalls. High doses may result in cracking of the exposed PMMA leaving random sidewall defects [7] while developer temperature and developer composition have been linked to sidewall cracking on the nanometer to micrometer scale [8]. In the absence of mask defects and under controlled exposure and development conditions, typical sidewall surface roughness is 30–50 nm [9].

The effects of x-ray radiation and development in the LIGA process have been discussed in several publications.

Schmalz *et al* studied the molecular weight and chemical degradation of PMMA and mode of action of development in GG developer solution [10–12]. They determined that the molar mass of PMMA is decreased and the chemical constitution of the polymer is changed enough that the end product of irradiated PMMA behaves differently, both physically and chemically, than the starting material. Henry *et al* investigated the structural changes of sheet PMMA that underwent x-ray exposure and found large variations in the volume change, or swelling, between samples from different vendors [13]. They determined that annealing the PMMA prior to exposure decreased the swelling observed after irradiation. Similarly, Moldovan looked at deformation and stress in PMMA from x-ray exposure over a wide range of exposure doses [7]. Here, cracking in the bulk exposed material was linked to random cracks on the sidewall, and a regular cracking pattern on the developed sidewall was attributed to mechanical loading which evolved during the development process. The swelling of patterned features on the top and bottom surfaces of sheet PMMA was tracked for various exposure doses resulting in an estimation of stress values due to gas accumulation and compaction. Pantenburg *et al* determined that decreased development temperature increases the contrast between exposed and unexposed PMMA. This research also showed that micro-holes may form inside sidewalls of crosslinked PMMA if secondary radiation from the mask deposits dose in the masked resist [14]. They also noted that room temperature development temperature decreases cracking at the substrate/PMMA interface. Under the same exposure conditions, MIBK/IPA developer produced sidewall cracks while GG developer did not [8]. De Carlo *et al* investigated bubbles and cracks in thick irradiated PMMA and found formation to be related to total dose as well as the average dose rate. Particularly, short pauses at the top and bottom of the exposure scan decreased the formation of bubbles in the irradiated PMMA [15]. Khan *et al* studied the causes for and the accumulation of gaseous species in the PMMA [16]. They noted that annealing reduced resist swelling and that x-ray spectral distribution greatly influenced the amount of swelling. In particular, that the degree of gaseous byproducts and swelling were related to the total dose deposited, the dose gradient in the sample and the dose deposition rate. Guimarães *et al* looked at sidewall quality and reached several conclusions: cracking begins during irradiation, several types of crack formations may appear, the time between exposure and development is critical in assessing the characteristics of cracks and dose profile and sample thickness are important in crack formation [17].

Most of the work above concentrated on samples with high top doses (greater than 10 kJ cm^{-3}) where bubbles form in the exposed area of the PMMA. Likewise, previous studies to address the effect of delayed development compared samples that were developed immediately after exposure to samples that were developed weeks after exposure [7, 17]. Neither bubble formation nor long delay times are desired or practical for routine processing.

The goal of this work is twofold: to determine factors influencing sidewall cracking and to define a processing window of dose and delay time to development where the quality of the PMMA mold is not compromised. This paper examines sidewall quality with an emphasis on conditions that would be applicable to routine processing of LIGA samples. Specifically, we examined sidewall cracking and its correlation to exposure dose and the delay between the end of exposure and the beginning of development. The x-ray exposure conditions used here did not result in any visible bubble formation in the irradiated PMMA. The delay times used in this work cover a wide range of delay times, from hours to days, at consistent intervals that are applicable to routine processing. We examined four delay times with three exposure doses and identified relationships between sidewall cracking, absorbed dose and delay between exposure and development.

2. Experimental details

PMMA sheets (Cyro, OP-1) 1.5–3 mm thick were annealed (ramp from 25 °C to 95 °C at 1 °C min^{-1}, hold at 95 °C for 6 h, cool to 25 °C at 0.5 °C min^{-1}), glued to substrates and then diamond fly-cut to the desired thickness. Final PMMA thicknesses of 1000 μm and 500 μm were used. The substrates were 100 mm diameter silicon wafers (1000 μm thick) coated with 6 μm of an aluminum alloy that was subsequently anodized [18].

X-ray exposures were carried out on beam lines 3.3.1 and 3.3.2 at the Advanced Light Source (ALS) located at Lawrence Berkeley National Laboratories, operating at 1.9 GeV ($E_c = 2.99$ KeV). The x-ray beam was filtered by 254 μm of beryllium, 5.6 μm of aluminum and either 130 mm of helium at 100 Torr (beam line 3.3.1) or 130 mm of air at atmospheric pressure (beam line 3.3.2). The x-ray mask consisted of a 100 μm thick silicon membrane patterned with a 34 μm gold absorber. This mask consisted of identical test patterns in each quadrant of the wafer. All samples were exposed using a scan rate of 15 mm s^{-1} and a scan length of 82 mm. The backside of the sample was cooled to 20 °C during the exposure. Samples were exposed to obtain three different bottom doses: 2.3, 2.7 and 3.2 kJ cm^{-3}. Bottom doses from 2 to 4 kJ cm^{-3} are typical for LIGA processing [8, 14, 19].

After exposure, the samples were cut into four quadrants using a dicing saw. This allowed four different delay experiments with exactly the same exposure conditions and pattern geometry. The cuts to dice the wafer were approximately 1 cm from the features analyzed. Sample pieces were placed in GG developer 4, 12, 24 and 72 h after the end of exposure [20]. Each sample was suspended with the resist facing down in fresh developer at 21.5 ± 0.2 °C. All solutions used in developing and rinsing were constantly agitated using a magnetic stirrer. All samples with identical exposure conditions were developed for the same time, regardless of delay, with the development time calculated using LEX-D [19]. After development the samples were rinsed in a mixture of diethylene glycol butyl ether (80%) and deionized (DI) water (20%) for 30 min followed by a DI water rinse for 30 min. The samples were allowed to air dry at room temperature. Table 1 summarizes the exposure and development parameters.

To analyze the sidewalls, the samples were diced through a series of developed negative square features ranging in sidewall widths from 150 μm to 2000 μm as shown by the dashed line in figure 1. SEM images of the developed features

Table 1. Sample conditions.

Sample number	Thickness (mm)	Bottom/top dose (kJ cm^{-3})	Delay (h)	Development time (h)
1	1000	2.3/4.2	4	72
2	1000	2.3/4.2	12	72
3	1000	2.3/4.2	24	72
4	1000	2.3/4.2	72	72
5	1000	2.7/5.0	4	48
6	1000	2.7/5.0	12	48
7	1000	2.7/5.0	24	48
8	1000	2.7/5.0	72	48
9	1000	3.2/6.1	4	36
10	1000	3.2/6.1	12	36
11	1000	3.2/6.1	24	36
12	1000	3.2/6.1	72	36
13	500	2.3/3.3	4	48
14	500	2.3/3.3	12	48
15	500	2.3/3.3	24	48
16	500	2.3/3.3	72	48
17	500	2.7/3.9	4	24
18	500	2.7/3.9	12	24
19	500	2.7/3.9	24	24
20	500	2.7/3.9	72	24
21	500	3.2/4.5	4	17
22	500	3.2/4.5	12	17
23	500	3.2/4.5	24	17
24	500	3.2/4.5	72	17

taken before and after dicing indicate that dicing did not introduce or increase the sidewall defects. The diced samples were mounted so that the sidewall surfaces of the square features could be examined using a Veeco Wyko NT3300 white light interferometer. The interferometer is capable of sub-nanometer vertical resolution. The samples were scanned using a 10× objective over the height of the PMMA wall to determine if there were any cracks. In samples that exhibited cracking, a scan with the 50× objective was performed toward the top of the PMMA structure to provide better resolution of the crack characteristics. The overall amount of sidewall cracking was determined using the 10× objective scan while the crack depths, the crack widths and the distance between cracks was determined from the 50× objective scans.

The results of the analysis will be presented using the following definitions and using the coordinate system in figure 1:

- Feature width F_w—feature extent in the x–y plane.
- Feature depth F_d—the thickness of the feature.
- Feature sidewall—the xz or yz plane of the developed feature. From figure 1, the sidewalls analyzed are parallel to the xz plane.
- Crack depth—the distance the crack extends into the PMMA (the y direction).
- Crack length—the linear extent of the crack on the surface of the PMMA sidewall (the x direction)
- Crack width—the width of the crack opening measured in the z direction.

3. Results

Figure 2 is an example of sidewall cracking in samples 5–8 from table 1 (2.7 kJ cm^{-3} bottom dose). The four scans represent the top 300 μm of PMMA in the 500 μm wide feature

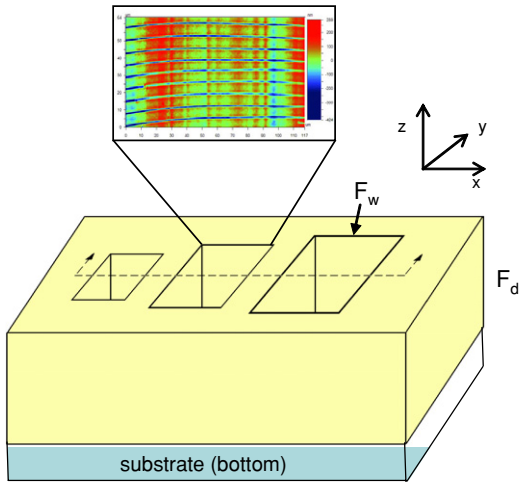

Figure 1. Schematic of the PMMA sample. The dashed line indicates where the sample was diced. Definitions in the text refer to the coordinate system defined in this figure.

(This figure is in colour only in the electronic version)

at each delay. The vertical striations are attributed to line edge roughness on the mask while the horizontal features are the fractures that appear if development is delayed. Typically, cracking is on the top of the feature and is very periodic. The cracks are generally parallel to the top surface of the PMMA as seen in figure 2 (12 h). The cracks curve down toward the corners of the square features and may end before reaching the adjoining sidewall. As the delay between the end of exposure and the beginning of development increases, the cracks encompass more of the feature sidewall (figure 2, 24 and 72 h); however, individual cracks toward the top of the feature are shorter than on features developed with a shorter delay as seen in figure 3.

The most significant variation in crack appearance is observed at higher doses and longer delays. Figure 4 is a 50× scan of the top 300 μm of a sidewall from sample 12. At the top of the structure, the cracks have a scale-like appearance. In the middle region, the fractures are longer and more linear. The bottom portion exhibits very evenly spaced and continuous horizontal cracks.

Only two of the 500 μm thick samples have any observable sidewall cracking, samples 20 and 24. Because the thinner resists show so little cracking, our reported results are all from the 1000 μm thick samples.

3.1. Extent of cracking

The extent of cracking is quantified here as the percentage of the sidewall, F_d, that exhibits cracks, i.e. if the top 400 μm of a 1000 μm thick sample has defects, it is said to have 40% cracking. Figure 5 is a plot of the average percentage of cracking as a function of development delay time for samples 1–12. The data show the average percentage of cracking for ten features from 150 μm to 2000 μm wide and the error bars represent one standard deviation. None of the samples developed within 4 h of exposure show evidence of any sidewall fractures. An increase in dose results in an increase in the extent of cracking as well as cracks appearing with shorter delay times.

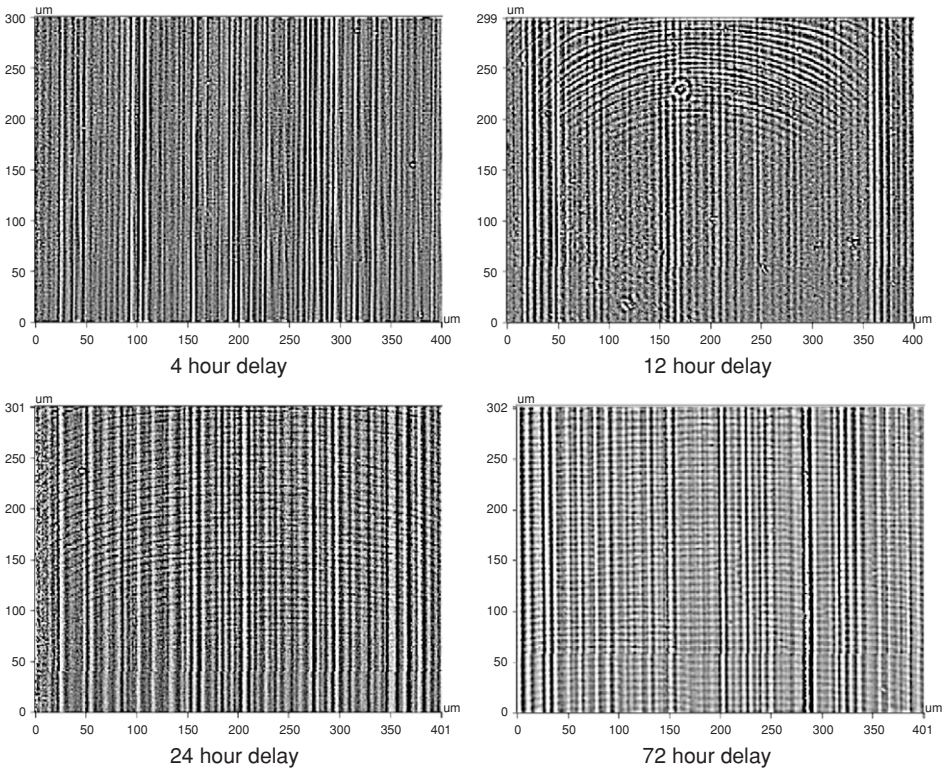

Figure 2. Examples of cracking for a 500 μm wide feature, 1000 μm thick, 2.7 kJ cm^{-3} bottom dose.

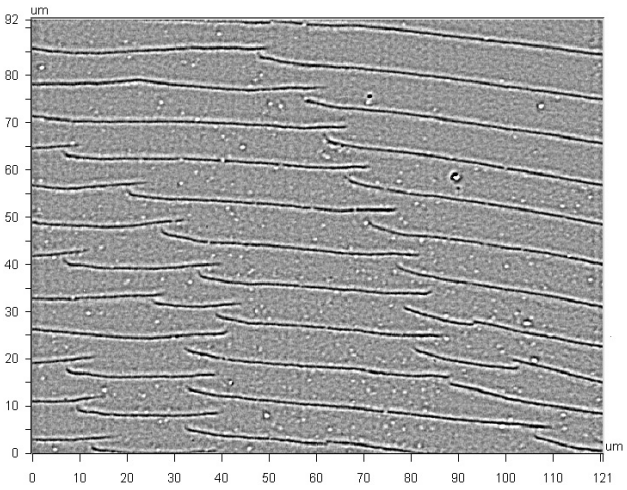

Figure 3. 50× surface scan using the 50× objective showing a close-up of cracking in the 24 h delay sample seen in figure 2.

Statistical analysis of the data (JMP software, SAS Institute, Cary, North Carolina) indicates that, in addition to dose and delay time, feature size is a statistically significant ($P < 0.05$) variable for sidewall cracking if the sizes of the features differ by greater than an order of magnitude. Figure 6 is a plot of the percentage of sidewall cracking versus development delay time for the 150 and 2000 μm features. It is evident that the large features exhibit more fracturing at shorter delay times; yet smaller features have more extensive cracking at longer delay times.

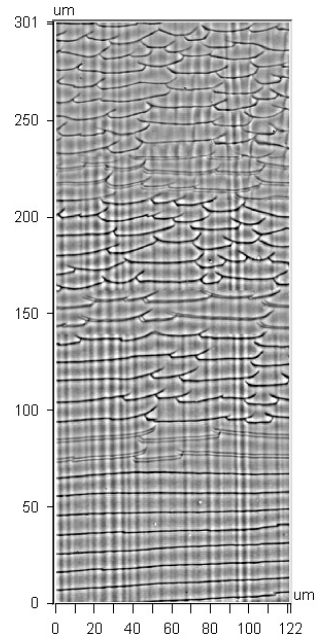

Figure 4. Sidewall surface topography of the center 122 μm of a 1000 μm wide feature from sample 12.

3.2. Crack depth and width

Crack depth was determined by reducing each column of pixels in the interferometer scan to a two-dimensional cross section as shown in figure 7. In figure 7, 'height' is the distance parallel to the xz plane of the feature and 'vertical position' is

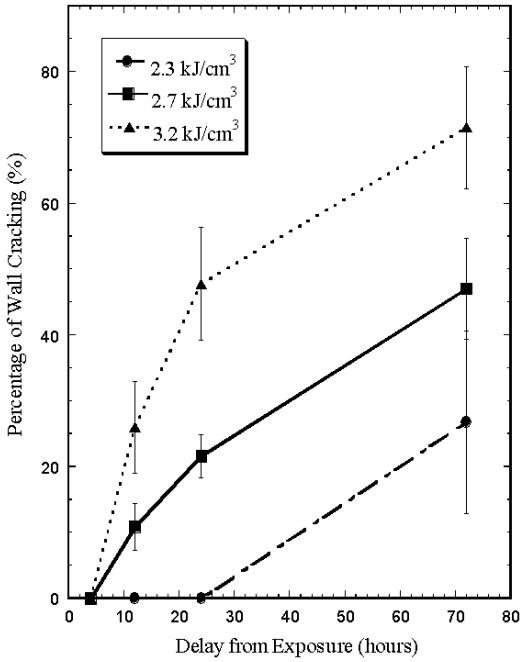

Figure 5. Percentage sidewall cracking versus delay time for three bottom doses. The error bars indicate the standard deviation in the measurement over feature sizes from 150 to 2000 μm.

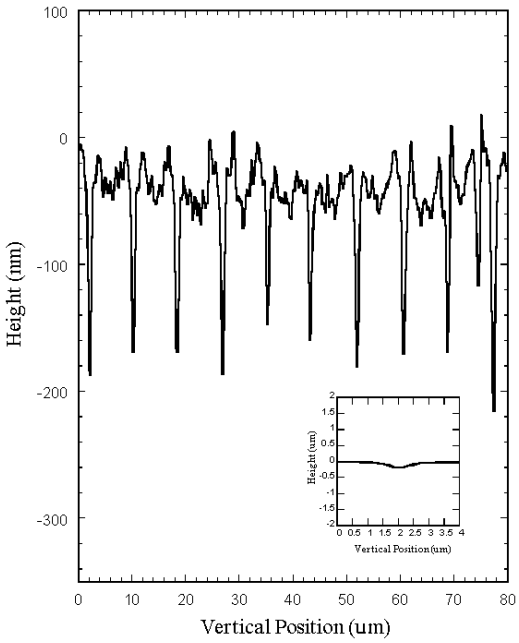

Figure 7. Cross-section profile of cracks in a 500 μm wide feature from sample 7. The inset is an enlargement of a single crack on a 1:1 x:y scale.

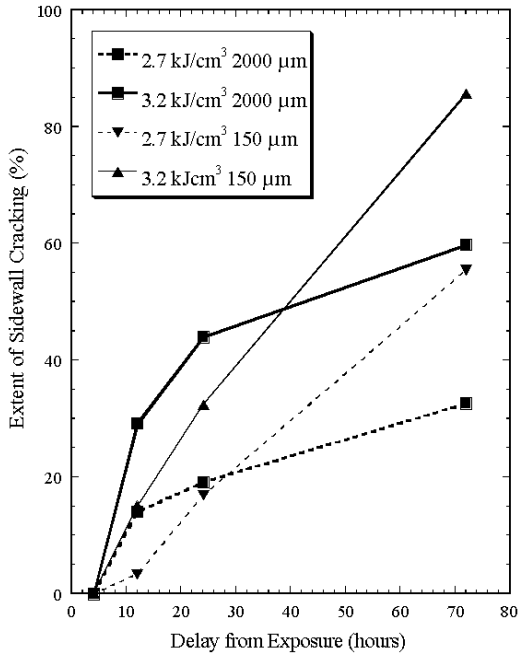

Figure 6. Percentage sidewall cracking versus delay time for 150 and 2000 μm wide features with bottom doses of 2.7 and 3.2 kJ cm^{-3}.

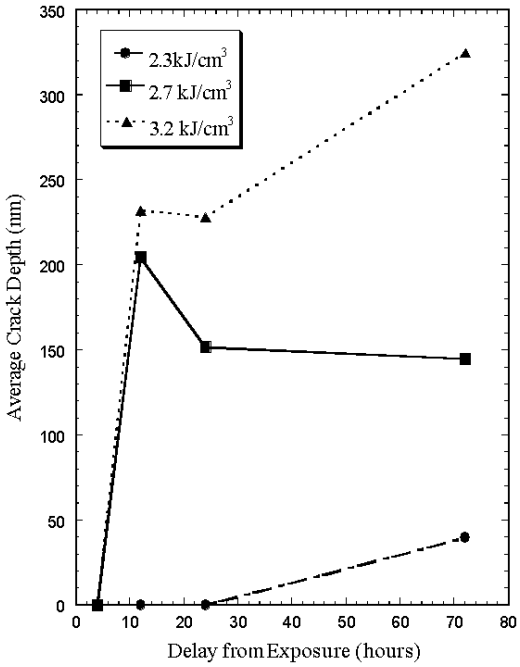

Figure 8. Average crack depth versus delay for three bottom doses (average of all feature sizes).

the distance from the top of the PMMA as defined in figure 1. For each feature, the difference between the mean plane height and all the crack minima is calculated for each column in the image and averaged to give a crack depth. The average depth of the cracks across all features, as a function of dose and delay from end of exposure, is shown in figure 8. In all cases, the cracks are shallow, less than 400 nm.

Figure 8 gives indication that the crack depth depends on dose. This is consistent with a radiation-damaged zone at the sidewall of the structure. During the x-ray exposure process, photoelectrons generated by the primary x-ray beam in the unmasked areas give rise to a secondary dose in the masked region, which diminishes rapidly with distance into the masked region. One micrometer into the masked region, a dose of 400 J cm^{-3} for the 3.2 kJ cm^{-3} samples and 300 J cm^{-3} for the 2.3 kJ cm^{-3} samples, is deposited. While making the transition from the exposed to the unexposed region, the gradients in

Table 2. Average crack width.

Dose (kJ cm^{-3})	Delay time			
	4 h	12 h	24 h	72 h
2.3	None	None	None	None
2.7	None	1.40 μm	1.35 μm	1.46 μm
3.2	None	1.92 μm	1.55 μm	1.54 μm

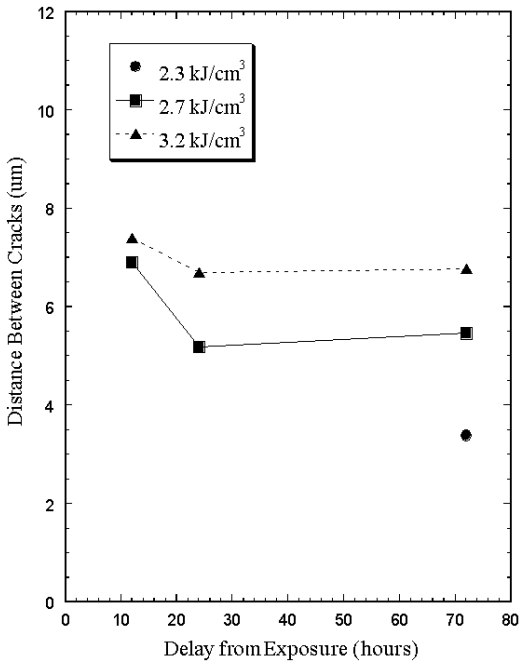

Figure 9. Distance between cracks versus delay for various doses (average of all feature sizes).

chemical and physical changes in the PMMA rapidly change in this region. Therefore, the crack shape may indicate a sudden increase in material strength between the exposed and unexposed regions.

The distance where the mean plane height intersects the crack on either side defines the crack width. For these samples, the width of a crack is much larger than its depth as illustrated in the inset in figure 7. Table 2 summarizes the crack width versus delay time for all three doses. Crack width appears to be essentially the same for all 1000 μm thick samples regardless of dose.

3.3. Distance between cracks

The distance between cracks is calculated by averaging the distance between the local minima in figure 7 over the entire 121 μm $\times$ 92 μm surface scan. Figure 9 suggests that the distance between cracks as an average for all feature sizes is a function of dose. 24 and 72 h delay times indicate a clear dependence of the distance between cracks on dose. Interestingly, the lower the dose, the shorter the distance between cracks.

4. Discussion

Two previous reports of sidewall cracking have focused on cracks similar to those described here [7, 17]. In those cases, the features under investigation were positive or free standing PMMA structures where fractures were concentrated on the corners of the structures but encompassed a larger portion of the sidewall at long delay times. Both studies concluded that the cracks were the result of a mechanical load but disagreed on when the cracks initiated. In this study, the sidewall is a negative PMMA feature which constrains the exposed PMMA and induces stress on the feature in different locations.

The morphologies of the cracks with the various delay times provide useful insight into a mechanism. If the cracks were present before development began, the crack characteristics would not change with delay time but the extent of the cracking would (see figure 2). Hence, this cannot be viewed as a growth process where the cracks grow or change over time, prior to development. Instead, the exposed PMMA contracts over time increasing the mechanical load on the sidewall. PMMA samples under tensile load are known to be susceptible to cracking in solvent [21, 22]. Hence, the developer induces cracking to relieve the stress at the interface. The cracking continues during development until a sub-critical stress is reached where crack formation is not possible. This is consistent with the first evidence of cracking occurring on the top of the structures. The periodic nature of the cracks is also consistent with a mechanical load on the sidewall.

The dependence of cracking on dose and delay is not unexpected given the explanation above. Increasing the dose increases the gaseous byproducts and material loss [10]. This results in greater extremes of expansion and contraction in the exposed region [7]. As the delay between the end of exposure and the beginning of development increases, there is more diffusion of gases and more relaxation of the polymer matrix and subsequent contraction in the exposed region.

From this work, it is possible to predict the range of conditions under which cracking in sidewalls may be avoided. The curves in figure 10 represent the calculated dose profiles for the three bottom doses used in this work for 1000 μm thick samples of PMMA. Overlaid are shapes that represent the average location that sidewall cracking ends for each of the dose profiles and delay times. These shapes represent the data from figure 5, converted from a percentage of sidewall cracking to an equivalent position where cracking no longer appears. From figure 10, we can conclude that cracking ends in specific dose ranges for a given delay. It appears that the low dose sample (bottom curve) is on the verge of cracking after a 24 h delay from exposure, although none was observed here. Figure 11 is a plot of delay time versus effective crack dose. Here, effective crack dose is defined as the dose deposited at the point where sidewall cracking ended and is represented by the intersection of a shape with the dose profile curve in figure 10. An empirical fit of the data in figure 11 yields the equation

$$\text{delay time} = 245\,000 \times \text{dose}^{-6.25}.$$

Areas that fall above this line indicate cracking while those below do not. Thus, to avoid sidewall cracking for a given top dose, the maximum development delay time can be predicted from the equation above.

In this study, only two 500 μm thick PMMA samples had any observable cracking, samples 20 and 24. Using the equation above and the applied top doses for the 2.7 and

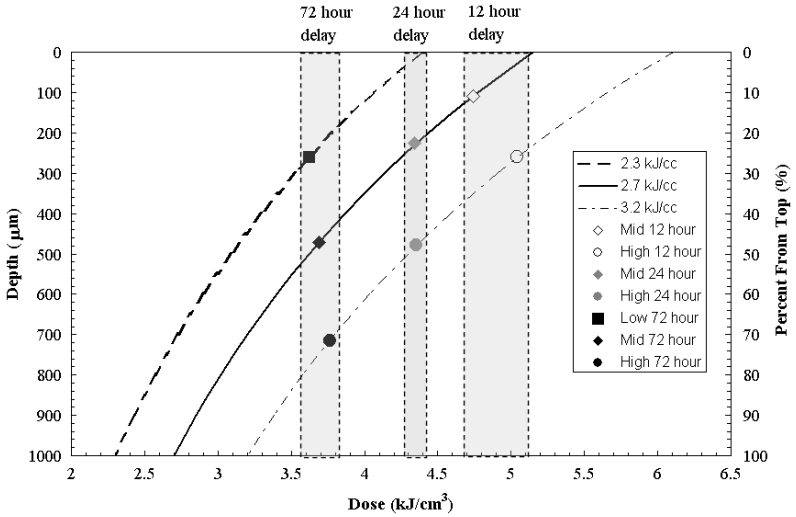

Figure10. Dose versus distance into PMMA (curves). Overlaid are shapes that represent the average distance from the top of the sample where cracking ends for each of the three dose profiles and their development delay times.

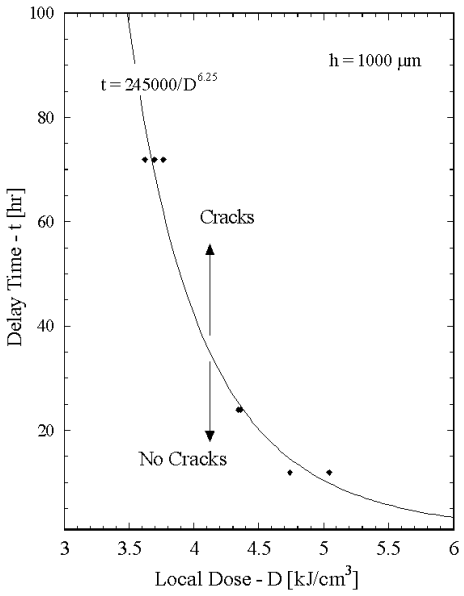

Figure 11. Local dose versus delay time. The curve represents a polynomial best fit of the data. The area above the curve represents when cracking will occur depending on the local deposited dose and the delay between exposure and development.

3.2 kJ cm^{-3} samples (3.9 and 4.5 kJ cm^{-3}, respectively), we would predict cracking with 50 and 20 h delay times, respectively. In fact, these samples displayed cracking with 72 h delay time in good agreement with the prediction. Since no delay times between 24 and 72 h were used in this study, we cannot determine if these samples would have displayed cracking at shorter delay times. The 2.3 kJ cm^{-3} sample did not have any cracking nor would cracking be expected until delay times in excess of 100 h.

It was shown by Henry *et al* that increased filtering of incoming radiation, effectively decreasing the top to bottom dose ratio, decreased the amount of PMMA swelling that occurred [13]. It has also been demonstrated that bubbling in PMMA and swelling can be reduced by adding delays at either end of the sample scan, thus allowing the gaseous byproducts of the exposed area extra time to diffuse. It should be noted that the data collected here represent a series of negative features with aspect ratio from 0.5 to 6.67. Higher aspect ratio features are expected to display higher cracking rates based on the trend in figure 5. It is possible that a more uniform dose-profile throughout the PMMA would alleviate sidewall cracking, especially for samples greater than 1 mm thick. However, there is a practical limit to x-ray filtering. Decreasing the top to bottom dose ratio increases exposure time and overall development time. Product requirements and the overall processing space need to be considered to produce features of the desired quality in the most economical way.

5. Conclusions

In order to better understand LIGA processing, we have examined PMMA sidewall cracking while varying PMMA thickness, dose and time delay between exposure and development. Cracking in sidewalls is most likely due to solvent-induced cracking of the sidewall during development. This condition is exacerbated by higher doses, longer delays and thicker material. These results lead to a simple predictive model and the following practical guidelines. Development should occur within 4 h of exposure in order to avoid any sidewall cracking due to exposure and development conditions. For lower doses and/or thinner resists, delay can be increased up to 12 h or more before cracking occurs. Further investigation into lower and higher doses, different dose profiles, smaller and different geometries and other PMMA thicknesses will greatly increase the understanding of processing space for using LIGA as a reliable micro-fabrication technique.

Acknowledgments

The authors would like to thank Stewart Griffiths, Neville Moody, Steve Goods, Georg Aigeldinger and Stan Mrowka

for their helpful discussions and thoughtful feedback. We would like to thank Cheryl Hauck, Kevin Krenz and Alf Morales for their processing assistance. We would also like to acknowledge the use of the Advanced Light Source in Berkeley, CA. The Advanced Light Source is supported by the Director, Office of Science, Office of Basic Energy Sciences, Materials Sciences Division, of the US Department of Energy under contract no. DE-AC03-76SF00098 at Lawrence Berkeley National Laboratory. Sandia National Laboratories is a multiprogram laboratory operated by Sandia Corporation, a Lockheed Martin Company, for the United States Department of Energy under contract DE-AC04-94-AL85000.

References

[1] Becker E W, Ehrfeld W, Hagmann P, Maner A and Mündmeyer D 1986 Fabrication of microstructures with high aspect ratios and great structural heights by synchrotron radiation lithography, galvanoforming, and plastic moulding (LIGA process) *Microelectron. Eng.* **4** 35–56

[2] Hagmann P, Ehrfeld W and Vollmer H 1987 Fabrication of microstructures with extreme structural heights by reaction injection molding *1st Meeting of the European Polymer Federation, European Symp. on Polymeric Materials (Lyon, France)* pp 241–51

[3] Moldovan N M, Mancini D C, Divan R, Makarova O V, Peele A and Podolak K R 2002 Side wall roughness in ultradeep x-ray lithography *Microsyst. Technol.* **9** 130–2

[4] Krenz K D, Aigeldinger G and Ceremuga J T 2004 Surface roughness evaluation of a LIGA micro component *19th Annual Meeting of the American Society for Precision Engineering*

[5] Aigeldinger G, Griffiths S K, Hachman J T, Morse D H, Skala D M, Talin A A and Yang C-Y P 2005 Evaluating mask substrate materials for deep x-ray lithography *High Aspect Ratio Micro Structure Technology Workshop (Gyeongju, Korea)* pp 96–7

[6] Achenbach S, Boerner M, Kinuta S, Bacher W, Mohr J and Saile V 2005 Structure quality in deep x-ray lithography applying commercial polyimide-based masks *High Aspect Ratio Micro Structure Technology Workshop (Gyeongju, Korea)* pp 112–3

[7] Moldovan N 1999 Deformation and stress in PMMA during hard x-ray exposure for deep lithography *Proc. SPIE Materials and Device Characterization in Micromachining II (Santa Clara, CA, USA)* vol 3875 pp 155–63

[8] Pantenburg F J, Achenbach S and Mohr J 1998 Characterisation of defects in very high deep-etch x-ray lithography microstructures *Microsyst. Technol.* **4** 89–93

[9] Rogner A, Eichner J, Munchmeyer D, Peters R-P and Mohr J 1992 The LIGA technique—what are the new opportunities? *J. Micromech. Microeng.* **2** 133–40

[10] Schmalz O, Hess M and Kosfeld R 1996 Structural changes in poly(methyl methacrylate) during deep-etch x-ray synchrotron radiation lithography: Part 2. Radiation effects on PMMA *Angew. Makromol. Chem.* **239** 79–91

[11] Schmalz O, Hess M and Kosfeld R 1996 Structural changes in poly(methyl methacrylate) during deep-etch x-ray synchrotron radiation lithography: Part 3. Mode of action of the developer *Angew. Makromol. Chem.* **239** 93–106

[12] Schmalz O, Hess M and Kosfeld R 1996 Structural changes in poly(methyl methacrylate) during deep-etch x-ray synchrotron radiation lithography: Part 1. Degradation of the molar mass *Angew. Makromol. Chem.* **239** 63–77

[13] Henry A C, McCarley R L, Das S, Khan Malek C and Phoche D S 1998 Structural changes in PMMA under hard x-ray irradiation *Microsyst. Technol.* **4** 104–9

[14] Pantenburg F J, Achenbach S and Mohr J 1998 Influence of developer temperature and resist material on the structure quality in deep x-ray lithography *J. Vac. Sci. Technol.* B **16** 3547–51

[15] De Carlo F, Mancini D C, Lai B and Song J J 1998 Characterization of exposure and processing of thick PMMA for deep x-ray lithography using hard x-rays *Microsyst. Technol.* **4** 86–8

[16] Khan C and Das S 2003 Swelling behaviour of poly(methylmethacrylate) thick resist layers in deep x-ray lithography *J. Synchrotron Radiat.* **10** 272–9

[17] Guimarães M S, Meyer P, Hahn L and Schulz J 2004 Preliminary results of fracture mechanics analysis on LIGA side wall quality *Microsyst. Technol.* **10** 722–7

[18] Griffiths S K *et al* 2005 Resist substrate studies for LIGA microfabrication with application to a new anodized aluminum substrate *J. Micromech. Microeng.* **15** 1700–12

[19] Griffiths S K 2004 Fundamental limitations of LIGA x-ray lithography: sidewall offset, slope and minimum feature size *J. Micromech. Microeng.* **14** 999–1011

[20] Glashauser W and Ghica G-V 1983 Method of stress-free development of irradiated polymethylmetacrylate, in http://www.uspto.gov/ *Patent number* 4,393,129 Germany: Siemens Aktiengeselschaft

[21] Bokoi Y, Ishiyama C, Shimojo M, Shiraishi Y and Higo Y 2000 Effects of sorbed water on crack propagation in poly(methyl methacrylate) under static tensile stress *J. Mater. Sci.* **35** 5001–11

[22] Arnold J C 1998 The effects of diffusion on environmental stress crack initiation in PMMA *J. Mater. Sci.* **33** 5193–204